Elastic scattering and breakup reactions of neutron-rich nucleus ^{11}Be on ^{208}Pb at 210 MeV

F. F. Duan,[1] Y. Y. Yang,[1,2,*] Jin Lei,[3,†] K. Wang,[1] Z. Y. Sun,[1,2] D. Y. Pang,[4] J. S. Wang,[5,1,2] X. Liu,[6] S. W. Xu,[1,2] J. B. Ma,[1] P. Ma,[1] Z. Bai,[1] Q. Hu,[1] Z. H. Gao,[1] X. X. Xu,[1,2] C. J. Lin,[7] H. M. Jia,[7] N. R. Ma,[7] L. J. Sun,[7,8] D. X. Wang,[7] G. Yang,[1,2] S. Y. Jin,[1,2] Z. Z. Ren,[3] Y. H. Zhang,[1,2] X. H. Zhou,[1,2] Z. G. Hu,[1,2] and H. S. Xu[1,2]
(RIBLL Collaboration)

[1]*CAS Key Laboratory of High Precision Nuclear Spectroscopy, Institute of Modern Physics, Chinese Academy of Sciences, Lanzhou 730000, China*
[2]*School of Nuclear Science and Technology, University of Chinese Academy of Sciences, Beijing 100080, China*
[3]*School of Physics Science and Engineering, Tongji University, Shanghai 200092, China*
[4]*School of Physics and Beijing Key Laboratory of Advanced Nuclear Materials and Physics, Beihang University, Beijing 100191, China*
[5]*School of Science, Huzhou University, Huzhou 313000, China*
[6]*Key Laboratory of Radiation Physics and Technology of the Ministry of Education, Institute of Nuclear Science and Technology, Sichuan University, Chengdu 610064, China*
[7]*Department of Nuclear Physics, China Institute of Atomic Energy, Beijing 102413, China*
[8]*School of Physics and Astronomy, Shanghai Jiao Tong University, Shanghai 200240, China*

(Received 13 January 2022; accepted 25 February 2022; published 7 March 2022)

Quasielastic scattering and breakup angular distributions for the neutron halo nucleus ^{11}Be on a ^{208}Pb target at the laboratory energy of 210 MeV, which corresponds to 5.2 times the Coulomb barrier, were measured at HIRFL-RIBLL (Heavy-Ion Research Facility in Lanzhou and Radioactive Ion Beam Line in Lanzhou). The quasielastic scattering angular distribution of ^{11}Be shows an obvious suppression of the Coulomb nuclear interference peak (CNIP) even at such a high incident energy. Theoretical results with the continuum discretized coupled channels (CDCC) method are in correspondence with the experimental data. The measured angular distribution of the ^{10}Be fragments is well reproduced considering elastic breakup contribution with the CDCC calculations plus nonelastic breakup contribution with the model of Ichimura, Austern and Vincent [Phys. Rev. C **32**, 431 (1985)]. The reduced reaction cross section of the ^{11}Be + ^{208}Pb system was compared with those of other reaction systems including tightly and weakly bound projectiles impinging on medium and heavy mass targets, where the former shows a significant enhancement. Systematical comparisons between the experimental data and theoretical calculations suggest that elastic scattering with heavy targets (such as ^{208}Pb) at relatively high incident energies is still sensitive to the structure of neutron-rich nuclei.

DOI: 10.1103/PhysRevC.105.034602

I. INTRODUCTION

Breakup reactions normally play an important role in the proton- and neutron-rich nuclei induced reactions due to the low separation energies, and have a large influence on the other channels such as elastic scattering [1–4]. For a two-body structured weakly bound projectile, the reaction process can be studied through a three body model, i.e., the continuum discretized coupled channels (CDCC) method. Experimentally, high quality data of elastic scattering angular distributions of this kind of projectile on light and heavy targets exhibit strong coupled channels effects at energies around the Coulomb barrier [1]. These effects can be interpreted by either the CDCC [5] or XCDCC [6] method. The latter is the extended version of CDCC, which takes into account dynamic core excitation. On the other hand, for three-body structured nuclei, like ^{11}Li, ^{14}Be, and ^{17}B [7], the breakup reaction is much more complicated; one has to use a four-body model [8] for these nuclei induced reactions.

^{11}Be, as a well known neutron halo nucleus with a strongly deformed core [9] and $S_n = 0.502$ MeV, has been widely studied [10]. In literature, many experiments using it as a projectile have been performed on both medium and heavy targets at low energies to investigate the effect of its exotic features through elastic scattering [11–17]. The elastic scattering angular distributions of all experiments with a ^{11}Be beam show a suppression of the Coulomb nuclear interference peak (CNIP) because of strong breakup coupling effects. Similar results were found in the elastic scattering of ^{6}He [18–22] and ^{11}Li [23] at energies close to the Coulomb barriers. In our previous work [24], the elastic scattering angular distribution of ^{11}Be + ^{208}Pb at 140 MeV was measured, and the same measurements for ^{9,10}Be + ^{208}Pb were simultaneously performed in this experiment. It has been found that the reaction cross section, which was extracted by the optical potential, of ^{11}Be is much larger than those of ^{9}Be and ^{10}Be. In addition, CDCC

*Corresponding author: yangyanyun@impcas.ac.cn
†Corresponding author: jinl@tongji.edu.cn

and XCDCC calculations reproduce quite well the elastic scattering angular distribution of ^{11}Be, with strong suppression of the CNIP, confirming that the strong breakup coupling effects still persist even at 3.5 times the Coulomb barrier. Besides, the angular and energy distributions of the ^{10}Be fragments from ^{11}Be breakup revealed that these fragments were mostly produced by the elastic breakup (EBU) mechanism in which all of the fragments remain in their ground states. In addition, nonelastic breakup (NEB) contributions, in which the valence neutron interacts nonelastically with the target, are also exhibited. The EBU calculation with CDCC plus NEB contributions using the Ichimura-Austern-Vincent (IAV) model [25] can well reproduce the data.

On the other hand, the elastic scattering of $^{8}\mathrm{B} + ^{208}\mathrm{Pb}$ at energies about three to four times the Coulomb barrier were also measured [26–28]. ^{8}B is one-proton halo nucleus, with a separation energy of $S_p = 0.136$ MeV. In Refs. [26–28], the elastic scattering angular distributions of ^{8}B, which exhibit the typical CNIP, are well reproduced by CDCC calculations. This is different from the case of one-neutron halo nucleus ^{11}Be on the ^{208}Pb target and at a similar energy around three times the Coulomb barrier [24]. In fact, the shape of the angular distribution for ^{8}B is more like the stable nucleus ^{6}Li on the same target [26]. The effect of coupling to the continuum of ^{8}B is much less than that of ^{11}Be. In addition, in Refs. [27,28] the reaction cross section for $^{8}\mathrm{B} + ^{208}\mathrm{Pb}$ is similar to that of $^{7}\mathrm{Be} + ^{208}\mathrm{Pb}$. The angular distribution of the ^{7}Be fragments from the ^{8}B breakup can be well reproduced by calculations which consider EBU plus NEB contributions. The origin of the different behaviors of proton and neutron halos was explained by the Coulomb and centrifugal barriers encountered by the valence proton in ^{8}B which suppress the coupling effects [29]. It is also suggested that the three times Coulomb barrier energy is not the reason for the modest effect of coupling to continuum observed in ^{8}B.

It is generally believed that when the incident energy is higher, the collision time will be shorter, and the multistep effects (such as those appearing in inelastic excitation) will become smaller [30]. Therefore, the measurements of the elastic scattering and breakup of the neutron-rich nuclei at higher energy are helpful to study the influence of breakup coupling effects on the elastic scattering angular distribution in depth. In this work, we report the measurement of the scattering of ^{11}Be on ^{208}Pb at an incident energy of 210 MeV (about 5.2 times the Coulomb barrier). The details about the experiment are introduced in Sec. II. The experimental results are analyzed in Sec. III. The comparison of the reduced total reaction sections for many systems is discussed in Sec. IV. The summary and conclusions are presented in Sec. V.

II. EXPERIMENT

The measurements were performed at the National Laboratory of Heavy Ion Research of the Institute of Modern Physics with a radioactive beam of ^{11}Be. The ^{13}C primary beam was delivered by the Heavy-Ion Research Facility in Lanzhou (HIRFL) [31,32] at 54.2 MeV/nucleon and impinged on a 4500-μm-thick ^{9}Be target. The ^{11}Be secondary beam was separated by the Radioactive Ion Beam Line in Lanzhou (RIBLL) [33,34] and transported to the experimental chamber by adjusting magnetic rigidity ($B\rho$). The schematic view of the detector setup in the chamber is shown in Fig. 1. Two double-sided silicon strip detectors (DSSDs) with thicknesses of 68 and 87 μm, labeled as Sistrip 1 and Sistrip 2, respectively, were installed 663 and 367 mm upstream from a 8.22-mg/cm^2-thick self-supporting ^{208}Pb target. The tracks of the incoming particles were determined by Sistrip 1 and Sistrip 2, from which the precise incident positions on the target were deduced. The ^{11}Be energy in the middle of the lead target was 210 MeV. A silicon detector array [35] was placed 300 mm downstream from the target. Three ΔE-E particle telescopes, labeled as Tel1, Tel2, and Tel3, were installed on the top, left, and right sides of the beam center, respectively. Each telescopic unit contained two stages: one DSSD as the ΔE detector, followed by one silicon detector (SD) as the E detector. Tel1 was placed at forward angles, covering an angular range from 7° to 26°. The DSSD in Tel1 consisted of 128 strips on both the junction and the ohmic sides, 157 μm thick, with an active area of 99.6 × 99.6 mm^2. In order to increase the geometric efficiency in the large-angle region, both Tel2 and Tel3 were placed in the large-angle area, covering the same angular range from 13° to 26°. The DSSDs in Tel2 and Tel3 were composed of 32 strips on both the junction and the ohmic sides, with 64 × 64 mm^2 of total active areas, 142 and 144 μm thick, respectively. The thicknesses of SDs in the three telescopes were 1499, 1528, and 1534 μm, respectively, with almost the same effective areas as the DSSDs.

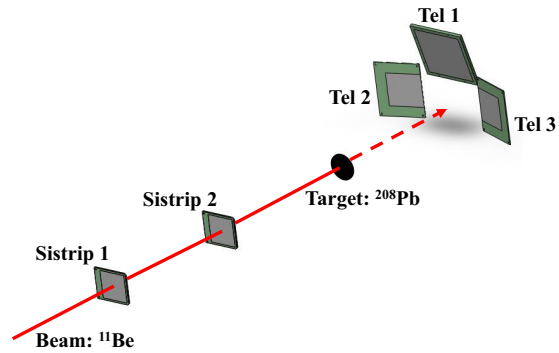

FIG. 1. Sketch of the detector setup.

A typical energy spectrum (E) for ^{11}Be obtained by the SD in Tel1 is shown in Fig. 2, from which two peaks, originating from elastically scattered ^{11}Be particles (peak1) and reaction products ^{10}Be (peak2), can be clearly separated. A Monte Carlo simulation was conducted to evaluate the Rutherford differential cross section. The ratio between the experimental elastic scattering and Rutherford differential cross section was obtained by $\frac{d\sigma(\theta)}{d\sigma_{\mathrm{Ruth}}(\theta)} = C \times \frac{N(\theta)_{\mathrm{exp}}}{N(\theta)_{\mathrm{Ruth}}}$. This method is free from the systematic errors of the calculation of the solid angles, the measured total number of incident particles, and target thickness. More details on descriptions of data analysis and detector misalignment correction are given in Refs [35–37].

III. RESULTS AND DISCUSSION

In order to investigate the impact of the breakup channel on the quasielastic scattering angular distributions in

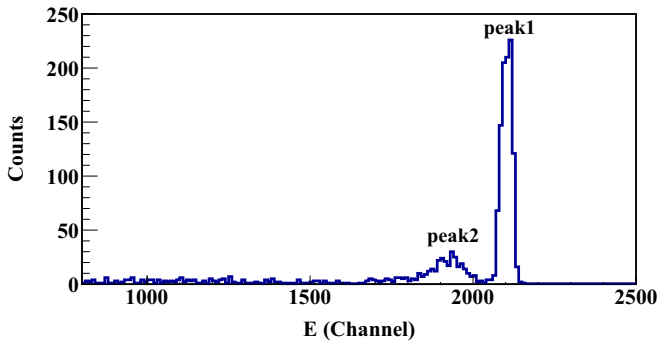

FIG. 2. One-dimensional energy spectrum for ^{11}Be on ^{208}Pb at 210 MeV obtained with the SD in Tel1. The two peaks correspond to the ^{11}Be from elastic scattering (peak1) and the ^{10}Be from breakup/transfer reaction (peak2).

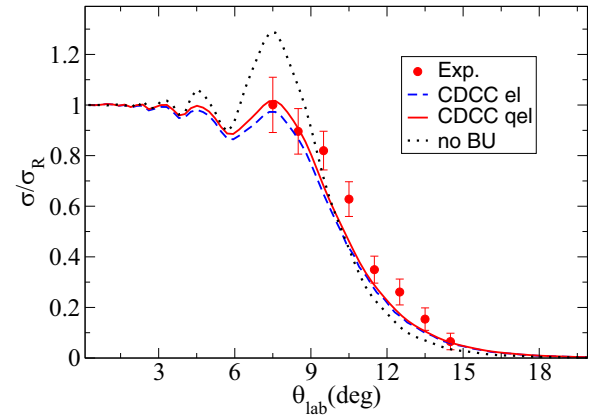

FIG. 3. The results of CDCC calculations and the experimental data of the quasielastic scattering of ^{11}Be + ^{208}Pb at $E_{\rm lab}$ = 210 MeV. The blue dashed, red solid, and black dotted curves are results of CDCC calculations of elastic and quasielastic scatterings and of no-continuum states, respectively.

the ^{11}Be + ^{208}Pb system, CDCC calculations have been performed using the computer code FRESCO [38]. The structure of ^{11}Be was assumed to be composed of a core ^{10}Be and a valence neutron. The spins of ^{10}Be were omitted. The n-^{10}Be binding potential was of Woods-Saxon form with parameters $r_0 = 2.585$ fm and $a_0 = 0.6$ fm, taken from Ref. [39]. The potential depth was adjusted to reproduce the binding energy of the n in the ground state, the first excited state ($1/2^-$; $E_x = 320$ keV), and the $E_x = 1.8$ MeV resonant state ($5/2^+_1$) of ^{11}Be [39]. The systematic single-folding nucleus-nucleus potential for ^{10}Be-target interactions [40] and the systematics of KD02 for n-target potentials [41] were used. In the calculation, the continuum states of the $n + ^{10}$Be system were discretized into bins up to a maximum excitation energy of $E_{\rm max} = 35$ MeV for each angular momentum ℓ between the valence neutron and the core ^{10}Be. The maximum value of ℓ is $\ell_{\rm max} = 6$. The model space we chose was large enough to ensure the convergence of the elastic scattering and breakup cross sections.

The experimental angular distribution of quasielastic scattering for ^{11}Be + ^{208}Pb and the calculated results are shown in Fig. 3. The error bars in the experimental cross sections are the statistical errors only. The CDCC calculations reproduce the data well over the full angular range. The red solid curve corresponding to the calculation result for the quasielastic scattering by considering the excited state of ^{11}Be reproduces better the data compared to the result considering the ^{11}Be ground state only (blue dashed line), of which the values of the standard minimum χ^2 are 1.75 and 2.35, respectively. The CNIP in both the experimental data and the calculations is obviously suppressed compared with the calculated result without continuum states (black dotted line). Similar results have been observed for the reactions of ^{11}Be + ^{208}Pb [24] at 3.5 times the Coulomb barrier and of ^{11}Be + ^{64}Zn [13] and ^{11}Be + ^{197}Au [15] at near-barrier energies. This phenomenon suggests that in the reaction of ^{11}Be + ^{208}Pb, even at energy of about 5 times the Coulomb barrier, strong breakup coupling effects still persist.

The modulus of the elastic scattering matrix (S-matrix) elements are shown in Fig. 4 as a function of the projectile-target orbital angular momentum. The behavior of the S-matrix elements at large angular momentum values reflects the long range absorption effects which have been widely discussed in the literature [12]. The low angular momentum part in which the modulus of the S-matrix has zero values shows the strong absorption effects.

In Fig. 5, we show the modulus of the scattering wave function computed by an optical potential, which can generate equally well the elastic scattering angular distribution by the CDCC calculation, in the xz plane. For that, we solve the two body Schrödinger equation in partial waves then sum them to get the scattering wave function in three dimensions. The two wings in the $z > 0$ range show the probability of finding the scattering particle in the forward angles, which is consistent with the results in Fig. 3. The black region near the origin shows the strong absorption effects, in which the scattering particle ^{11}Be is absorbed by the target nucleus ^{208}Pb forming the compound nucleus, confirming the findings in Fig. 4. Remember that the scattering wave function is the sum of a spherical wave and a plane wave, and the plane wave

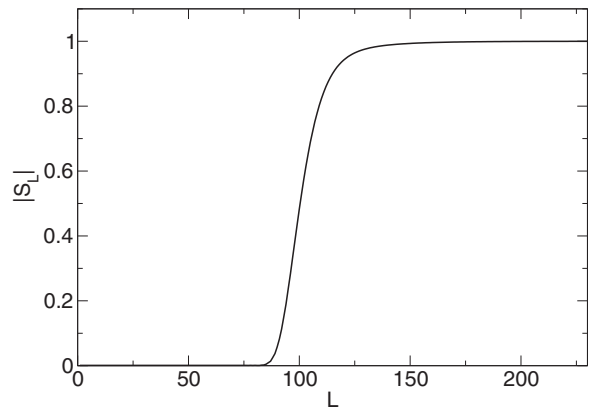

FIG. 4. Modulus of the elastic S matrix as a function of the angular momentum for ^{11}Be + ^{208}Pb.

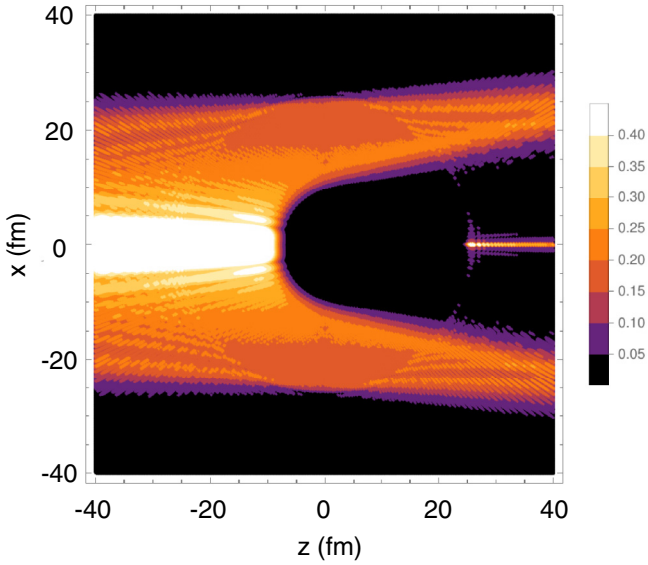

FIG. 5. Modulus of the scattering wave function of ^{11}Be + ^{208}Pb in the xz plane.

contribution explains the results in the region of $\theta \approx 0$ in the forward direction.

In this experiment, the ^{10}Be fragments, probably stemming from the breakup/transfer processes, were clearly identified. The computed ^{10}Be angular distributions in Fig. 6 suggest the CDCC calculation (red dash-dotted line) fails to reproduce the data for $\theta_{lab} \gtrsim 7°$. This result, which is due to the CDCC method accounting only for the EBU mechanism, is also consistent with the findings of Refs. [13,15,24]. The ignored NEB contribution (cyan dashed line in Fig. 6) can be computed using the model proposed by Ichimura, Austern, and Vincent (IAV) [42], which has been successfully applied in experiments on elastic scattering of ^{11}Be and ^{8}B [13,15,24,28]. With the NEB contribution superposed on the EBU result, the sum (green line in Fig. 6) is in rather good agreement with

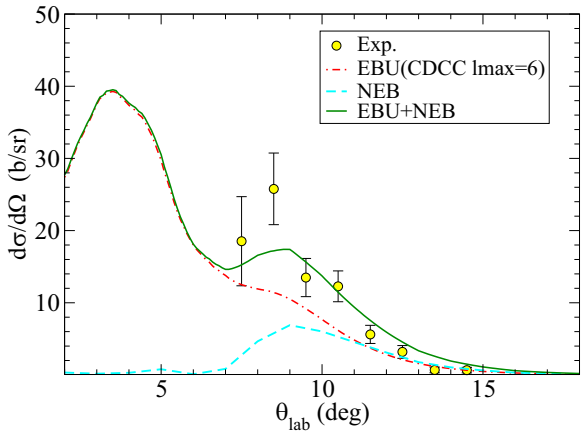

FIG. 6. Experimental breakup differential cross section, as a function of the ^{10}Be laboratory scattering angle, for the ^{11}Be + ^{208}Pb system at $E_{lab} = 210$ MeV compared with the calculations. See text for the details.

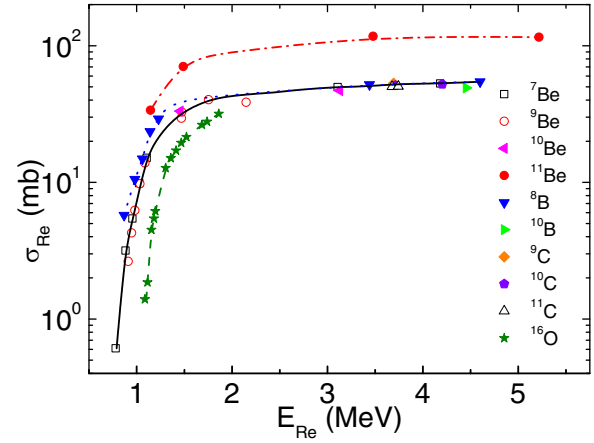

FIG. 7. Reduced reaction cross sections for several projectiles on several medium- to heavy-mass targets. The curves are to guide the eye.

the data. Similarly to previous results on ^{11}Be + ^{208}Pb at an incident energy of 140 MeV [24], the Coulomb breakup is the dominant function in reactions with heavy targets.

From the analysis of the elastic scattering angular distribution, the reaction cross section of ^{11}Be + ^{208}Pb at 210 MeV deduced from CDCC calculation is 7678 mb. Comparisons of the reaction cross sections for weakly and tightly bound systems can provide information about possible influences of the breakup and transfer channels of light weakly bound nuclei on elastic scattering. Here, a widely used reduction method [43] was performed. The procedures were to divide the reaction cross section by $(A_P^{1/3} + A_T^{1/3})^2$ and the incident energy by $Z_P Z_T/(A_P^{1/3} + A_T^{1/3})$, where A_P (A_T) and Z_P (Z_T) are the mass and charge numbers of the projectiles (targets). In this way, the normal geometrical and charge differences between reaction systems were properly minimized without washing out the dynamical effects of interest [43].

The results, shown in Fig. 7, involve systems of tightly and weakly bound nuclei on medium and heavy targets. The reduced reaction cross section for the ^{11}Be + ^{208}Pb system obtained in this work was compared with those using different projectiles (Be, B, C, and O projectiles). The reaction cross sections were taken from Ref. [44] for the ^{7}Be + ^{58}Ni system; Refs. [27,28] for ^{7}Be + ^{208}Pb; Ref. [45] for ^{9}Be + ^{120}Sn; Ref. [24] for ^{9}Be + ^{208}Pb; Ref. [11] for ^{10}Be + ^{64}Zn; Ref. [24] for ^{10}Be + ^{208}Pb; Ref. [11] for ^{11}Be + ^{64}Zn; Ref. [14] for ^{11}Be + ^{120}Sn; Ref. [24] for ^{11}Be + ^{208}Pb; Ref. [44] for ^{8}B + ^{58}Ni; Refs. [27,28] for ^{8}B + ^{208}Pb; Ref. [46] for ^{10}B + ^{208}Pb; Ref. [27] for ^{9}C + ^{208}Pb; Ref. [46] for ^{10}C + ^{208}Pb; Ref. [46] for ^{11}C + ^{208}Pb; and Ref. [47] for ^{16}O + ^{64}Zn. The tightly bound and weakly bound nuclei reaction systems all present larger reduced cross sections compared to the benchmark of stable double magic nucleus ^{16}O. The reduced cross sections for the p-halo nucleus ^{8}B barely show any obvious enhancements with respect to the weakly bound "normal" nuclei (^{7,9,10}Be, ^{10}B, ^{9,10,11}C) at energies above the Coulomb barrier. However, the ones for the n-halo nucleus ^{11}Be are obviously larger under the same conditions.

It can be clearly seen that the results for ^{11}Be at $E_{\mathrm{Re}} =$ 1.488, 3.478 and 5.217 MeV are 70.47, 117.4 and 115.6 mb, respectively, which are inconsistent with the asymptotic value of 50.0 mb for weakly bound and exotic nuclei [48]. This indicates that the loose structure of ^{11}Be makes a great contribution at such high incident energies. This, in fact, also exhibits the additional channels coupling effects on the reaction cross sections in ^{11}Be are still strong. The experimental results show breakup reaction is of importance, and, simultaneously, NEB has a non-negligible influence on data analysis.

IV. SUMMARY

In this paper, we reported new experiment data on the quasielastic scattering and breakup reactions of ^{11}Be on ^{208}Pb at an incident energy of $E_{\mathrm{lab}} = 210$ MeV, corresponding to about 5.2 times the Coulomb barrier. The quasielastic scattering angular distribution of $^{11}\mathrm{Be} + {}^{208}\mathrm{Pb}$ shows obvious suppression in the CNIP area, which is the same as in other ^{11}Be experiments in Refs. [13,15,24]. CDCC calculations have been performed and well reproduce the quasielastic data, indicating that the coupled channels effects in this reaction system persist even at such a high incident energy. The breakup cross section in $^{11}\mathrm{Be} + {}^{208}\mathrm{Pb}$ has also been measured. The angular distribution of ^{10}Be is underestimated at angles beyond 7° by CDCC calculations. The result of the NEB contribution which has been calculated by the IAV model [42] plus the EBU contribution by CDCC reproduces well the experiment data. These calculations imply that the EBU mechanism is the main cause of producing ^{10}Be fragments. In addition, the NEB process should not be neglected.

The reaction cross section for $^{11}\mathrm{Be} + {}^{208}\mathrm{Pb}$, by reduction method, was compared with other projectiles, including the proton halo ^{8}B nucleus, on medium- to heavy-mass targets. It is observed that the values of σ_{Re} for tightly bound or weakly bound nuclei systems are larger than that for ^{16}O. Reactions with the n-halo projectile ^{11}Be have reaction cross sections much higher than those of ^{8}B reaction systems in the energy region above the Coulomb barrier. This difference indicates that the additional channels' couplings on the reaction cross sections in n-halo nucleus ^{11}Be systems are larger than other systems at higher incident energies.

ACKNOWLEDGMENTS

We would like to acknowledge the staff of HIRFL for the operation of the cyclotron and their friendly collaboration. This work was financially supported by the National Natural Science Foundation of China (No. 11575256, No. 12105330, No. 12035011, No. 11975167, No. 12105204, and No. U2067205), and the Youth Innovation Promotion Association CAS (No. 2020411). J.L. is partially supported by the Fundamental Research Funds for the Central Universities. The project was funded by the Key Laboratory of High Precision Nuclear Spectroscopy, Institute of Modern Physics, Chinese Academy of Sciences.

[1] N. Keeley, R. Raabe, N. Alamanos, and J. L. Sida, Prog. Part. Nucl. Phys. **59**, 579 (2007).
[2] N. Keeley, N. Alamanos, K. Kemper, and K. Rusek, Prog. Part. Nucl. Phys. **63**, 396 (2009).
[3] L. F. Canto, P. R. S. Gomes, R. Donangelo, J. Lubian, and M. S. Hussein, Phys. Rep. **596**, 1 (2015).
[4] J. Kolata, V. Guimarães, and E. Aguilera, Eur. Phys. J. A **52**, 123 (2016).
[5] G. H. Rawitscher, Phys. Rev. C **9**, 2210 (1974).
[6] R. de Diego, J. M. Arias, J. A. Lay, and A. M. Moro, Phys. Rev. C **89**, 064609 (2014).
[7] Z. Ren and G. Xu, Phys. Lett. B **252**, 311 (1990).
[8] T. Matsumoto, E. Hiyama, M. Yahiro, K. Ogata, Y. Iseri, and M. Kamimura, in Proceedings of the 8th International Conference on Clustering Aspects of Nuclear Structure and Dynamics [Nucl. Phys. A **738**, 471 (2004)].
[9] H. G. Bohlen, T. Dorsch, T. Kokalova, W. von Oertzen, C. Schulz, and C. Wheldon, Phys. Rev. C **75**, 054604 (2007).
[10] M. Lyu, Z. Ren, H. Horiuchi, B. Zhou, Y. Funaki, G. Röpke, P. Schuck, A. Tohsaki, C. Xu, and T. Yamada, Eur. Phys. J. A **57**, 51 (2021).
[11] A. Di Pietro, G. Randisi, V. Scuderi, L. Acosta, F. Amorini, M. J. G. Borge, P. Figuera, M. Fisichella, L. M. Fraile, J. Gomez-Camacho, H. Jeppesen, M. Lattuada, I. Martel, M. Milin, A. Musumarra, M. Papa, M. G. Pellegriti, F. Perez-Bernal, R. Raabe, F. Rizzo *et al.*, Phys. Rev. Lett. **105**, 022701 (2010).
[12] A. Di Pietro, V. Scuderi, A. M. Moro, L. Acosta, F. Amorini, M. J. G. Borge, P. Figuera, M. Fisichella, L. M. Fraile, J. Gomez-Camacho, H. Jeppesen, M. Lattuada, I. Martel, M. Milin, A. Musumarra, M. Papa, M. G. Pellegriti, F. Perez-Bernal, R. Raabe, G. Randisi *et al.*, Phys. Rev. C **85**, 054607 (2012).
[13] A. Di Pietro, A. Moro, J. Lei, and R. de Diego, Phys. Lett. B **798**, 134954 (2019).
[14] L. Acosta, M. A. G. Álvarez, M. V. Andrés, M. J. G. Borge, M. Cortés, J. M. Espino, D. Galaviz, J. Gómez-Camacho, A. Maira, I. Martel, A. M. Moro, I. Mukha, F. Pérez-Bernal, E. Reillo, D. Rodríguez, K. Rusek, A. M. Sánchez-Benítez, and O. Tengblad, Eur. Phys. J. A **42**, 461 (2009).
[15] V. Pesudo, M. J. G. Borge, A. M. Moro, J. A. Lay, E. Nácher, J. Gómez-Camacho, O. Tengblad, L. Acosta, M. Alcorta, M. A. G. Alvarez, C. Andreoiu, P. C. Bender, R. Braid, M. Cubero, A. Di Pietro, J. P. Fernández-García, P. Figuera, M. Fisichella, B. R. Fulton, A. B. Garnsworthy *et al.*, Phys. Rev. Lett. **118**, 152502 (2017).
[16] M. Mazzocco, C. Signorini, M. Romoli, A. De Francesco, M. Di Pietro, E. Vardaci, K. Yoshida, A. Yoshida, R. Bonetti, A. De Rosa, T. Glodariu, A. Guglielmetti, G. Inglima, M. La Commara, B. Martin, D. Pierroutsakou, F. Sandoli, M. nd Soramel, L. Stroe, N. Kanungo, R. nd Khai, T. Motobayashi *et al.*, Eur. Phys. J. A **28**, 295 (2006).
[17] M. Mazzocco, C. Signorini, M. Romoli, R. Bonetti, A. De Francesco, A. De Rosa, M. Di Pietro, L. Fortunato, T. Glodariu,

A. Guglielmetti, G. Inglima, T. Ishikawa, H. Ishiyama, R. Kanungo, N. Khai, S. Jeong, M. La Commara, B. Martin, H. Miyatake, T. Motobayashi *et al.*, Eur. Phys. J.: Spec. Top. **150**, 37 (2007).

[18] E. F. Aguilera, J. J. Kolata, F. M. Nunes, F. D. Becchetti, P. A. DeYoung, M. Goupell, V. Guimarães, B. Hughey, M. Y. Lee, D. Lizcano, E. Martinez-Quiroz, A. Nowlin, T. W. O'Donnell, G. F. Peaslee, D. Peterson, P. Santi, and R. White-Stevens, Phys. Rev. Lett. **84**, 5058 (2000).

[19] O. Kakuee, J. Rahighi, A. Sánchez-Benítez, M. Andrés, S. Cherubini, T. Davinson, W. Galster, J. Gómez-Camacho, A. Laird, M. Lamehi-Rachti, I. Martel, A. Shotter, W. Smith, J. Vervier, and P. Woods, Nucl. Phys. A **728**, 339 (2003).

[20] A. Di Pietro, P. Figuera, F. Amorini, C. Angulo, G. Cardella, S. Cherubini, T. Davinson, D. Leanza, J. Lu, H. Mahmud, M. Milin, A. Musumarra, A. Ninane, M. Papa, M. G. Pellegriti, R. Raabe, F. Rizzo, C. Ruiz, A. C. Shotter, N. Soić *et al.*, Phys. Rev. C **69**, 044613 (2004).

[21] A. M. Moro, K. Rusek, J. M. Arias, J. Gómez-Camacho, and M. Rodríguez-Gallardo, Phys. Rev. C **75**, 064607 (2007).

[22] L. Acosta, A. M. Sánchez-Benítez, M. E. Gómez, I. Martel, F. Pérez-Bernal, F. Pizarro, J. Rodríguez-Quintero, K. Rusek, M. A. G. Alvarez, M. V. Andrés, J. M. Espino, J. P. Fernández-García, J. Gómez-Camacho, A. M. Moro, C. Angulo, J. Cabrera, E. Casarejos, P. Demaret, M. J. G. Borge, D. Escrig *et al.*, Phys. Rev. C **84**, 044604 (2011).

[23] M. Cubero, J. P. Fernández-García, M. Rodríguez-Gallardo, L. Acosta, M. Alcorta, M. A. G. Alvarez, M. J. G. Borge, L. Buchmann, C. A. Diget, H. A. Falou, B. R. Fulton, H. O. U. Fynbo, D. Galaviz, J. Gómez-Camacho, R. Kanungo, J. A. Lay, M. Madurga, I. Martel, A. M. Moro, I. Mukha *et al.*, Phys. Rev. Lett. **109**, 262701 (2012).

[24] F. Duan, Y. Yang, K. Wang, A. Moro, V. Guimarães, D. Pang, J. Wang, Z. Sun, J. Lei, A. Di Pietro, X. Liu, G. Yang, J. Ma, P. Ma, S. Xu, Z. Bai, X. Sun, Q. Hu, J. Lou, X. Xu *et al.*, Phys. Lett. B **811**, 135942 (2020).

[25] M. Ichimura, N. Austern, and C. M. Vincent, Phys. Rev. C **34**, 2326 (1986).

[26] Y. Y. Yang, J. S. Wang, Q. Wang, D. Pang, J. B. Ma, M. R. Huang, J. L. Han, P. Ma, S. L. Jin, Z. Bai, Q. Hu, L. Jin, J. B. Chen, N. Keeley, K. Rusek, R. Wada, S. Mukherjee, Z. Y. Sun, R. F. Chen, X. Y. Zhang *et al.*, Phys. Rev. C **87**, 044613 (2013).

[27] Y. Y. Yang, X. Liu, D. Y. Pang, D. Patel, R. F. Chen, J. S. Wang, P. Ma, J. B. Ma, S. L. Jin, Z. Bai, V. Guimarães, Q. Wang, W. H. Ma, F. F. Duan, Z. H. Gao, Y. C. Yu, Z. Y. Sun, Z. G. Hu, S. W. Xu, S. T. Wang *et al.*, Phys. Rev. C **98**, 044608 (2018).

[28] K. Wang, Y. Y. Yang, A. M. Moro, V. Guimarães, J. Lei, D. Y. Pang, F. F. Duan, J. L. Lou, J. C. Zamora, J. S. Wang, Z. Y. Sun, H. J. Ong, X. Liu, S. W. Xu, J. B. Ma, P. Ma, Z. Bai, Q. Hu, X. X. Xu, Z. H. Gao *et al.* (RIBLL Collaboration), Phys. Rev. C **103**, 024606 (2021).

[29] Y. Y. Yang, X. Liu, and D. Y. Pang, Phys. Rev. C **94**, 034614 (2016).

[30] S. Ogawa, T. Matsumoto, Y. Kanada-En'yo, and K. Ogata, Phys. Rev. C **104**, 044608 (2021).

[31] J. Xia, W. Zhan, B. Wei, Y. Yuan, M. Song, W. Zhang, X. Yang, P. Yuan, D. Gao, H. Zhao, X. Yang, G. Xiao, K. Man, J. Dang, X. Cai, Y. Wang, J. Tang, W. Qiao, Y. Rao, Y. He *et al.*, Nucl. Instrum. Methods Phys. Res., Sect. A **488**, 11 (2002).

[32] W. Zhan, J. Xia, H. Zhao, G. Xiao, Y. Yuan, H. Xu, K. Man, P. Yuan, D. Gao, X. Yang, M. Song, X. Cai, X. Yang, Z. Sun, W. Huang, Z. Gan, and B. Wei, Nucl. Phys. A **805**, 533c (2008), special issue, iNPC 2007.

[33] W. L. Zhan, J. R. Dang, Q. M. Yin, B. W. Wei, J. C. Wang, X. W. Meng, Z. Y. Guo, R. R. He, Y. X. Luo, Z. Y. Sun, S. H. Jiang, W. S. Zhang, Q. J. Wang, G. H. Liu, S. X. Zhou, Y. F. Wang, G. Q. Xiao, J. X. Li, and L. J. Qing, Sci. China Ser. A Math. **42**, 528 (1999).

[34] Z. Y. Sun, W. L. Zhan, Z. Y. Guo, G. Q. Xiao, and J. X. Li, Nucl. Instrum. Methods Phys. Res., Sect. A **503**, 496 (2003).

[35] F.-F. Duan, Y.-Y. Yang, B.-T. Hu, J.-S. Wang, Z.-H. Gao, X.-Q. Liu, D. Patel, P. Ma, J.-B. Ma, S.-Y. Jin, Z. Bai, Q. Hu, G. Yang, X.-X. Sun, N. Ma, L.-J. Sun, H. Jia, X.-X. Xu, and C. Lin, Nucl. Sci. Tech. **29**, 165 (2018).

[36] Y. Yang, J. Wang, Q. Wang, J. Ma, M. Huang, J. Han, P. Ma, S. Jin, Z. Bai, Q. Hu, L. Jin, J. Chen, R. Wada, Z. Sun, R. Chen, X. Zhang, Z. Hu, X. Yuan, X. Cao, Z. Xu *et al.*, Nucl. Instrum. Methods Phys. Res., Sect. A **701**, 1 (2013).

[37] F.-F. Duan, Y.-Y. Yang, D.-Y. Pang, B.-T. Hu, J.-S. Wang, K. Wang, G. Yang, V. Guimarães, P. Ma, S.-W. Xu, X.-Q. Liu, J.-B. Ma, Z. Bai, Q. Hu, S.-Y. Jin, X.-X. Sun, J.-S. Yao, H.-K. Qi, and Z.-Y. Sun, Chin. Phys. C **44**, 024001 (2020).

[38] I. J. Thompson, Comput. Phys. Rep. **7**, 167 (1988).

[39] P. Capel, G. Goldstein, and D. Baye, Phys. Rev. C **70**, 064605 (2004).

[40] Y. P. Xu and D. Y. Pang, Phys. Rev. C **87**, 044605 (2013).

[41] A. Koning and J. Delaroche, Nucl. Phys. A **713**, 231 (2003).

[42] M. Ichimura, N. Austern, and C. M. Vincent, Phys. Rev. C **32**, 431 (1985).

[43] P. R. S. Gomes, J. Lubian, I. Padron, and R. M. Anjos, Phys. Rev. C **71**, 017601 (2005).

[44] E. F. Aguilera, E. Martinez-Quiroz, D. Lizcano, A. Gómez-Camacho, J. J. Kolata, L. O. Lamm, V. Guimarães, R. Lichtenthäler, O. Camargo, F. D. Becchetti, H. Jiang, P. A. DeYoung, P. J. Mears, and T. L. Belyaeva, Phys. Rev. C **79**, 021601(R) (2009).

[45] A. Arazi, J. Casal, M. Rodríguez-Gallardo, J. M. Arias, R. Lichtenthäler Filho, D. Abriola, O. A. Capurro, M. A. Cardona, P. F. F. Carnelli, E. de Barbará, J. Fernández Niello, J. M. Figueira, L. Fimiani, D. Hojman, G. V. Martí, D. Martínez Heimman, and A. J. Pacheco, Phys. Rev. C **97**, 044609 (2018).

[46] Y. Y. Yang, J. S. Wang, Q. Wang, D. Y. Pang, J. B. Ma, M. R. Huang, P. Ma, S. L. Jin, J. L. Han, Z. Bai, L. Jin, J. B. Chen, Q. Hu, R. Wada, S. Mukherjee, Z. Y. Sun, R. F. Chen, X. Y. Zhang, Z. G. Hu, X. H. Yuan *et al.*, Phys. Rev. C **90**, 014606 (2014).

[47] C. Tenreiro, J. C. Acquadro, P. A. B. Freitas, R. Liguori Neto, G. Ramirez, N. Cuevas, P. R. S. Gomes, R. Cabezas, R. M. Anjos, and J. Copnell, Phys. Rev. C **53**, 2870 (1996).

[48] J. J. Kolata and E. F. Aguilera, Phys. Rev. C **79**, 027603 (2009).